Dual Band Low Profile Capacitively Coupled Beam Steerable Square Loop Antenna

Arpan Pal, *Student member, IEEE,* Amit Mehta, *Senior member, IEEE*, Dariush Mirshekar-Syahkal, *Senior member, IEEE*, Prafulla Deo, *member IEEE*, Hisamatsu Nakano, *Life Fellow, IEEE*

Abstract—A dual band low profile switched beam Square Loop Antenna (SLA) fed by capacitively coupled feeding mechanism is presented. Two square loops are excited by four rectangular feeding patches which are fed with vertical probes. The capacitively coupled feeding arrangement introduces capacitance into the antenna input impedance and cancels the high inductance due to close proximity of ground plane and feeding probes. This feeding technique enables the antenna to be matched to 50Ω feed line and helps in the realization of low profile SLA. The antenna has a height of 3.04mm; i.e. $\lambda_0/26$ for the operating frequency of 3.8GHz. The Dual Band Capacitively Coupled Square Loop Antenna (DBCCSLA) is developed for covering 3.8 GHz and 4.7 GHz frequency bands and each band possesses an impedance bandwidth of 120 MHz. In both frequency bands when any of the four ports is excited, keeping other ports open circuited, the antenna generates a tilted beam directed away from the excited port, having a maximum directivity of 9.3 dBi. By exciting ports one at a time the antenna can steer its tilted beam in four different quadrants to scan the entire space in front of antenna.

Index Terms—Impedance matching, low profile antenna, square loop antenna, capacitively coupled feed, beam steering, dual band antenna.

I. INTRODUCTION

The recent portable transceivers (smart phones, PDAs and tablet devices) are expected to have low profile structures, small size and high data rate transmission capability. Because of their ability to transmit and receive signals from the intended direction, the beam steerable antennas are highly desirable for portable wireless devices. These antennas can evade the noise source and possess high signal to noise ratio (S/N). Consequently, they enable high data rate transmission and reception.

Currently some wireless networks use multi element phased array antennas [1]-[2] in their base station for beam steering application, but these antennas are not suitable for portable handheld devices due to their limited available spaces. Therefore, the implementation of steerable antennas in these modern devices would need a single element steerable antenna with a simple feeding mechanism. The first few ideas of single element beam steerable antennas were proposed as early as in 2003 [3]-[4], and since then have gained significant attention in antenna research community. A variety of geometries [5]-[9] have been investigated to realize single element beam steerable antennas. However, these antennas cannot be easily integrated with the other frontend RF electronics normally because of

their thick structures. For example, the square loop antenna (SLA) [8]-[9] reported for beam steering applications has a thickness of quarter wavelength ($\lambda_g/4$ where λ_g being guide wavelength in dielectric substrate). This limitation is due to the fact that the radiated field from the reverse image of the electric current on the square loop tends to cancel out the radiated field of the square loop current itself if the conducting ground plane is placed in a close proximity to the square loop. The close proximity of the conducting ground plane results in a significant increase in the stored electromagnetic energy which increases the antenna quality factor (Q) and decreases the impedance bandwidth. In this condition the matching of the antenna input impedance to a resistive (e.g. 50Ω) feeding port is difficult over a wide bandwidth. To overcome this problem High Impedance Surface (HIS) [10] and Perfectly Magnetic Conductors (PMC) surface [11] have been utilized. These artificial surfaces allow the antenna to be placed in a very close proximity to the ground plane as the image of the antenna current in HIS and PMC surfaces is in-phase with the actual antenna current and the radiated fields add-up in space. Further, Hybrid High Impedance Surface (HHIS) [12] has been reported for thickness reduction of beam steerable SLA. The HHIS reduces the height of SLA from $\lambda_0/4$ [9] to $\lambda_0/13.7$ [12]. However, the SLAs using HHIS surfaces uses numerous vias which can make them bulky and heavy, and more complex to manufacture.

The main challenge in designing low profile conventional SLA is the matching of the antenna input impedance to the 50Ω feed line. In this paper, a capacitively coupled feeding mechanism is presented for achieving the input impedance matching. This capacitive coupling introduces appropriate capacitance into the antenna input impedance, cancelling out the high inductance due to the feeding probe and close proximity of the ground plane. Thus, the new feeding mechanism allows the radiating square loop to be placed very close to the conducting ground plane. The proposed Capacitively Coupled Square Loop Antenna (CCSLA) is similar to [13]-[14] and has a net substrate thickness of 3.04 mm (i.e.: $\lambda_0/26$) at the operating frequency.

Compared to [12] the CCSLA achieves a 47% reduction in substrate thickness without using any band gap structure. Hence, the structure of CCSLA is lighter in weight, cheaper and simpler to fabricate. However, the CCSLA pays a price of its low profile by having a narrow operating bandwidth.

In this work, first the impedance bandwidth of the low profile CCSLA has been increased by loading the square loop with narrow gaps. This loading provides two close-by resonances [15]. These two resonances are merged to obtain a

broader impedance bandwidth. The work is then extended to develop a low profile dual loop Dual Band CCSLA (DBCCSLA) antenna. The two operating bands are 3.8 GHz and 4.7 GHz and the antenna is truly dual band, i.e. in both bands it is beam steerable. These bands find applications in defense and security, point-to-point and point-to-multipoint applications, satellite communications, radar system, WiMAX, etc.

This paper has three main sections. In section II, using impedance curves it is explained why SLA fails to resonate when is brought in close proximity with the ground plane. In section III, a step-by-step detailed study on the design of the low profile gap loaded CCSLA is presented. And in section IV, the design of the dual loop dual band DBCCSLA consisting of two co-centered square loops capacitively coupled to the feed line is presented. The antenna performances are simulated using CST Microwave studio based on Finite Integration Technique in Time Domain (FIT-TD) [16]. The antenna prototypes have been fabricated using standard photolithography and characterized by using a Vector Network Analyzer (VNA). The radiation patterns are measured using Satimo's StarLab [17].

II. EFFECTS OF GROUND PLANE PROXIMITY ON SLA RESONANCE

Fig. 1 shows four ports coaxial fed tilted beam steering SLA. This is the conventional SLA similar to one presented in [9]. The SLA is developed using Rogers 4350B substrate having permittivity $\varepsilon_r = 3.48$ and side length L=80 mm. The square loop is composed of four conducting strips each having a length of l=34.5 mm and a width of w=1 mm. As the resonance frequency of SLA is inversely proportional to its average circumferential length [18], the mean perimeter of 134 mm (4 × ($l-w$)) gives rise to a resonance at 4.7 GHz. The antenna has a thickness of $h \approx 11$mm which is a quarter of the wavelength in the dielectric of the substrate ($\lambda_g \approx \lambda_0/\{(\varepsilon_r+1)/2\}^{1/2}$) at the operating frequency (4.7 GHz). The antenna is fed from the bottom by four vertical conducting probes which touch the loop at points A, B, C and D. The probes have a diameter of 1.3 mm.

Fig 2(a) shows the reflection co-efficient of the SLA for two thicknesses (h_1) when port $A_{0,rf}$ is excited and the remaining ports (B_0, C_0 and D_0) are open circuited. When the thickness is 11 mm ($\approx \lambda_g/4$) the antenna resonates properly at 4.7 GHz with an impedance bandwidth of 400 MHz. However, when the thickness of the antenna is reduced to 3.04 mm ($\approx \lambda_0/21$) with all other parameters fixed the antenna stops resonating at the test frequency. This effect which is due to the close proximity of the ground plane increases the input impedance in general and in particular introduces a high inductance into the antenna input impedance. This fact can be vividly seen by the impedance curves for two thicknesses in Fig 2(b).

(a) Top view

(b) Side view
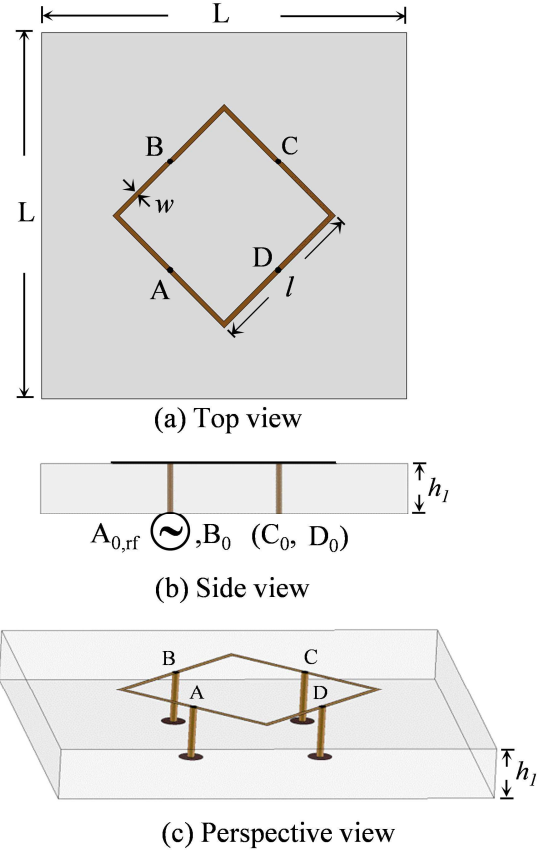
(c) Perspective view

Fig. 1. Top, side and perspective views of the probe fed square loop antenna (SLA).

It can be seen that for the operating frequency of 4.7GHz and antenna thickness 11 mm the input impedance of the SLA is 41+j4Ω. Since the reactance is close to zero the input impedance is approximately resistive, equal to 41Ω. This enables a close enough matching of the antenna input impedance to the 50Ω feed line in a straightforward manner and provides a good resonance behavior. This fundamental resonance of the conventional SLA is designated as 'unloaded mode' [15]. As with [8]-[9], this unloaded mode produces a tilted beam pointing away from the feeding point.

However, for thickness 3.04 mm the input impedance of the SLA shoots up to 260 + j217Ω, due to close proximity of ground plane and cause the impedance mismatch. This stops the resonance and entails reduced efficiency and gain of the antenna.

To tackle this problem, a capacitively coupled feeding technique [13]-[14] is developed to match the thin substrate SLA to the 50Ω feed line. The capacitive coupled feeds introduce appropriate capacitance into the input impedance of the antenna. This cancels the high inductance of the impedance and at the same time reduces the overall input impedance value close to a 50 Ω. To emphasize, this feeding mechanism enables the radiating square loop to be placed very close to the ground plane with little effects on the radiation efficiency and operating frequency of 4.7 GHz. This concept is presented next.
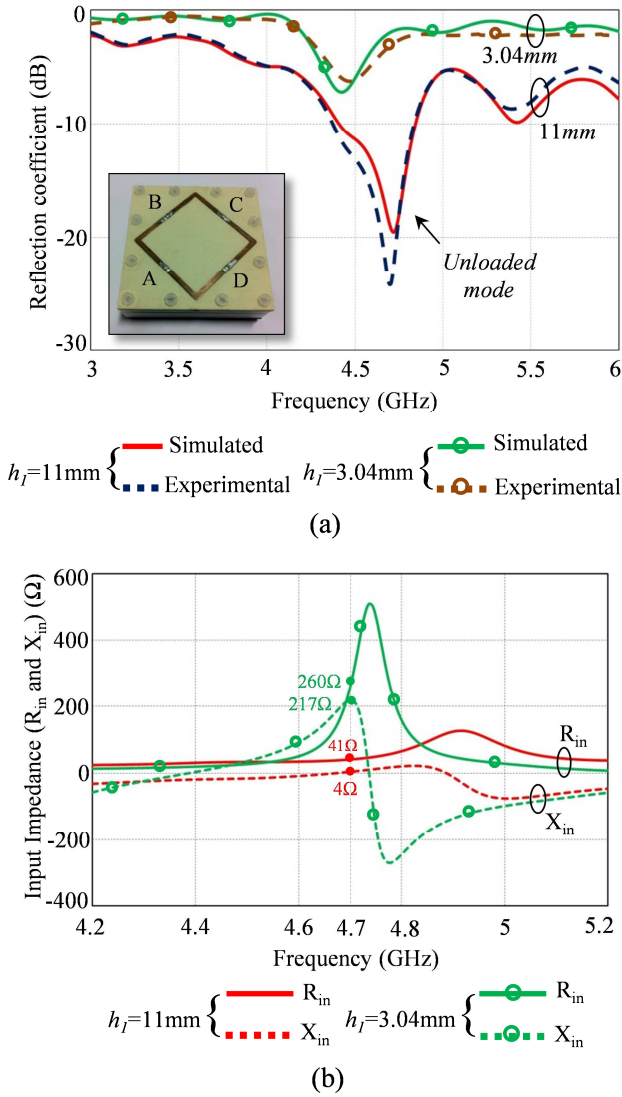
Fig. 2. (a) Reflection coefficients, (*inset*) prototype and (b) Input impedances of the conventional SLA simulated for different substrate thickness h_l.

III. THICKNESS REDUCTION OF SQUARE LOOP ANTENNA USING CAPACITIVELY COUPLED FEEDING

Fig. 3 shows the top, side and zoom views of H =3.04 mm thick Capacitively Coupled Square Loop Antenna (CCSLA) developed for the operating frequency of 4.7 GHz. For ease of fabrication, the square loop is etched on the top surface of two stacked Rogers 4350B substrate (permittivity ε_r=3.48, loss tangent $tan\delta$ =0.004), each having an area of L × L = 80mm × 80 mm and a thickness of h = 1.52 mm. The whole structure is backed by a conducting metal ground plane.

The unique feature of this SLA is that instead of directly feeding the radiating loop as in Fig. 1, it is capacitively coupled to the 50Ω feedline probes by four rectangular feeding patches (A_P, B_P, C_P and D_P). The patches are placed on the top of the substrate on the four outer sides of the loop. They are placed

parallel to the loop arm with the centre of patch aligning with the middle of each arm. The patches are connected to four bottom ports ($A_{0,rf}$, B_0, C_0 and D_0) with the four vertical conducting probes each having a diameter of 1.3 mm. These probes are connected at the centre of the respective feeding patches at the top.

(a) Top view

(c) Zoom view

(b) Side view
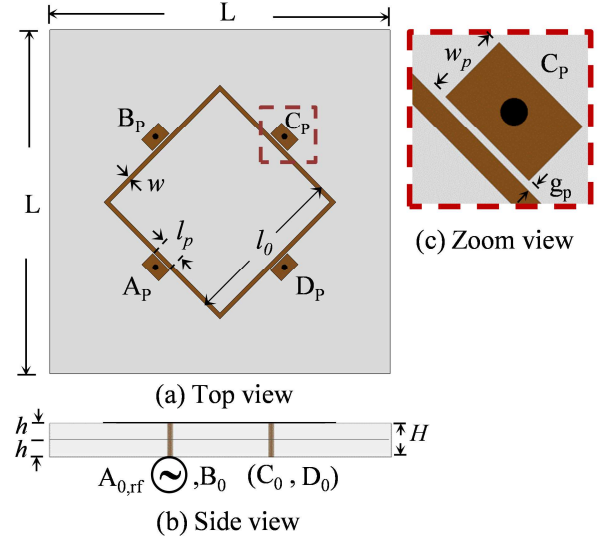
Fig. 3. Top, side and zoom views of the single loop CCSLA with a substrate thickness of 3.04 mm.

Each patch has a length of l_p = 5.6 mm and a width of w_p= 3.6 mm, and is separated from the radiating square loop by an optimised gap distance of g_p = 0.35 mm. The square loop has four conducting arms, each having end to end length l_0= 38.6 mm and width w=1 mm. The average circumferential length [$4\times(l_0-w)$] of the square loop is selected to 150.4 mm. All of these parameters were obtained using the CST optimizer for attaining a resonance at 4.7 GHz.
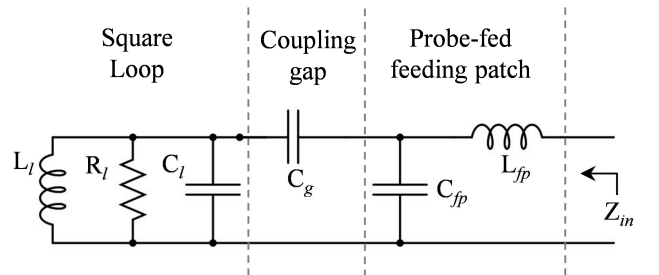
Fig. 4. Equivalent circuit model of CCSLA

Fig. 4 shows the equivalent circuit model of the CCSLA. The equivalent model of the square loop antenna is basically a parallel tuned circuit for the square loop operating in the resonant frequency and consists of well-known parallel combination of *RLC* elements. These values of the square loop (R_l, L_l, and C_l) can be calculated from the equations given in [18]. The rectangular feeding patch can be treated as a parallel plate capacitance (C_{fp}) and the probe feed can be represented by an inductive reactance element (L_{fp}) in series with the C_{fp} [19].

A series capacitance, C_g represents the coupling gap between the feeding patch and the square loop and can be calculated by spectral domain method [20].The above circuit is an impedance transformer. Therefore by choosing correct dimensions for the feeding patch and the gap between the patch and antenna, the impedance of the antenna at the excitation location can be transformed to a range of input impedances at the feed. The input impedance of the equivalent circuit model of the CCSLA mathematically can be expressed as:

$$Z_{in} = \left(\left(\left(\left(\frac{1}{R_l} + \frac{1}{j\omega L_l} + j\omega C_l \right)^{-1} + \frac{1}{j\omega C_g} \right)^{-1} + j\omega C_{fp} \right)^{-1} + j\omega L_{fp} \right)$$

(1)

Using the expressions given in [18]-[20] the theoretical values for each of the elements (R, L, C) were calculated. Table. 1 shows these calculated values of the equivalent circuit element at the two resonant frequencies of 4.7 GHz and 3.8 GHz.

Table. 1. Calculated model parameters of the CCSLA.

Resonant frequency (GHz)	4.7	3.8
Antenna dimensions (mm)	l_0=38.6 w=1 l_p=5.6 w_p=3.6 g_p=0.35	l_0=48.5 w=1 l_p=5 w_p=3.18 g_p=0.5
R_l (Ω)	49	60
L_l (nH)	0.0459	0.05
C_l (pF)	25	35.2
C_g (pF)	10	9.6
C_{fp} (pF)	0.01	0.008
L_{fp} (nH)	0.2	0.2
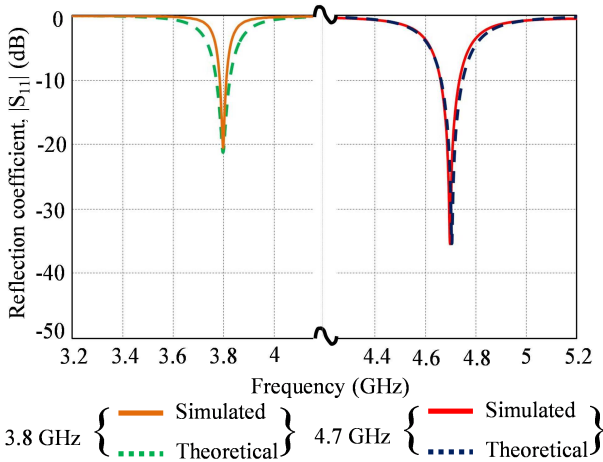
Fig. 5. Simulated and theoretical reflection coefficients of CCSLA for the two dimensions given in Table. 1

The input impedance model in equation (1) was implemented using MATLAB for two different geometry sets of CCSLA with the dimensions given in Table. 1. The reflection coefficient characteristics obtained from the CST simulations and MATLAB model are compared in Fig. 5. It can be seen that the theoretical equivalent circuit model is in good agreement with the simulated results.
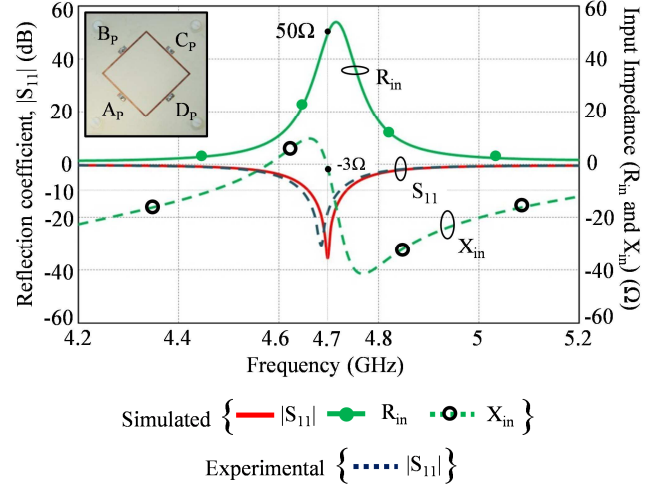
Fig. 6. Reflection coefficients and input impedances of the CCSLA for substrate thickness H=3.04mm. (*inset*) prototype.

Fig. 6 shows the reflection coefficient and input impedance of the new low profile CCSLA. It can be seen that at the operating frequency the input reactance (X_{in}= −3Ω) is close to zero and the net impedance is virtually resistive, equal to 50Ω. This enables a good match to the feed line and as a result the antenna resonates efficiently at 4.7 GHz, as shown in Fig. 5. Therefore, the capacitive coupling can introduce adequate capacitance into the antenna input impedance to eliminate the high inductance due to close proximity of the loop to the ground plane and also can reduce the overall impedance for satisfactory matching of the antenna input impedance with 50Ω coaxial feed line. However, this is achieved at an expense of reduced impedance bandwidth. In fact, the low profile CCSLA offers an impedance bandwidth of only 80 MHz compared to 400 MHz for the conventional SLA, Fig. 1, with height = 11 mm.

For expanding the bandwidth the ability of the square loop to resonate at a set of modes is exploited [21]. In [15], [22], it is shown that if a gap loading is made in the radiating square loop, in addition to the unloaded resonance(s) it provides supplementary 'loaded resonances'. These loaded and unloaded modes occur in sets and in close proximity with each other. Moreover, these loaded modes have similar radiation patterns [15] as that of unloaded modes. In this work, firstly loaded mode is extracted and then is merged with unloaded mode for broadening the impedance bandwidth.

Fig. 7 shows the reflection coefficients of the CCSLA with gaps loaded at different locations on the radiating square loop. As alluded earlier, the capacitive excitation of the conventional SLA by feeding patches leads to a resonance at 4.7 GHz (which

is associated with the unloaded mode when there are no gaps) and a narrow impedance bandwidth of 80 MHz. When an arbitrary gap of length g=1 mm was introduced at the middle of the square loop arm adjacent to the feeding patch A_P, the antenna resonance (4.7 GHz) was found to be unchanged.
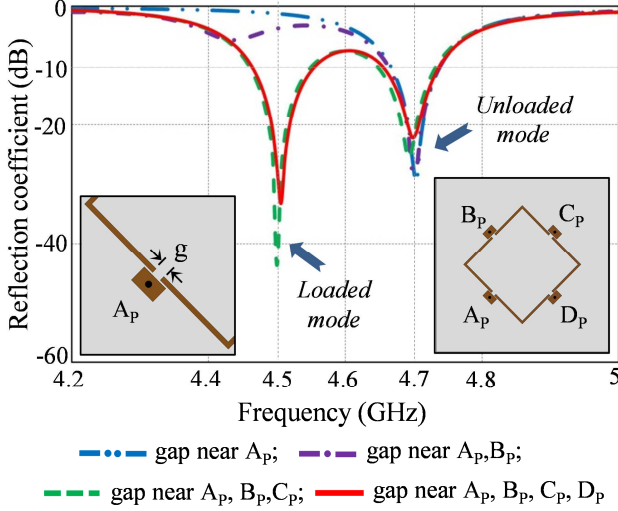
Fig. 7. Reflection coefficients of the CCSLA with loaded gap cut at different positions in the square loop.

Further, when a 2nd gap also of length g was inserted in the middle of the square arm adjacent to patch B_P, an additional but small loaded resonance was observed at 4.4 GHz. Next when a 3rd gap g was inserted adjacent to C_P, a stronger loaded resonance at 4.5 GHz is observed. In this case the individual bandwidths for both modes were 100 MHz each. And finally, when a 4th gap was inserted in the arm adjacent to feeding patch D_P, it was found that resonances of both modes at 4.5 GHz and 4.7 GHz remained unchanged. The inset of Fig. 6 shows top view of antenna when all 4 gaps are in place. In this work for bandwidth expansion we choose the 4 gaps design as it preserves the structure symmetry. Next and last part of this section is about merging both of these modes together by varying the size of the loading gap.
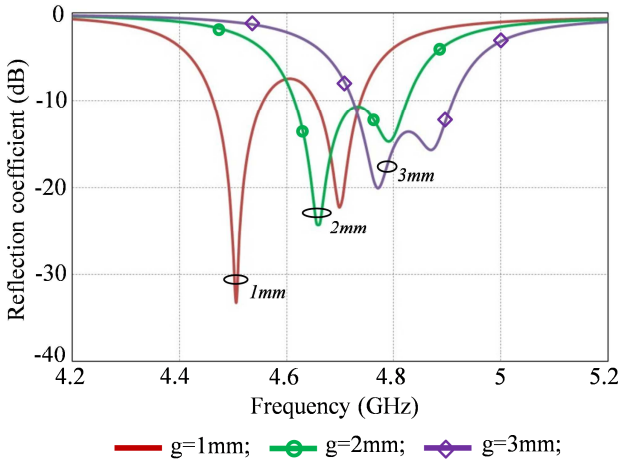
Fig. 8. Effect of the gap length on the reflection coefficient of the CCSLA.

The effect of varying g on the reflection coefficient of the CCSLA, keeping the rest of the dimensions fixed, is shown in Fig. 8. As seen in this figure, an increase in g effectively reduces the average circumferential length of the square loop. As a result both of the resonances shift to the higher frequencies. More importantly with the increase in g the frequency shift of the 'loaded mode' is more than that of the 'unloaded mode'. As a result, their corresponding (−10 dB) bandwidths merge together as $g \geq 2$ mm, providing a broader impedance bandwidth for the CCSLA. This phenomenon is clearly seen for $g = 2$ and 3 mm. For this reason in the design in Section IV, a gap of size 2.7 mm was selected which offered a combined bandwidth of 240 MHz.
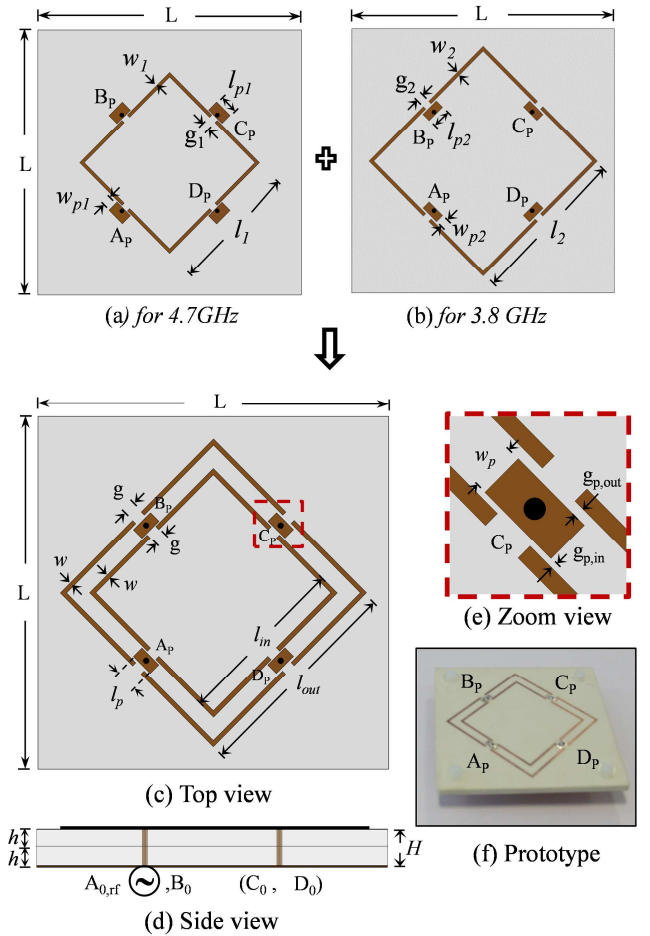
Fig. 9. (a) Top view of the CCSLA operating at 4.7 GHz. (b) Top view of the CCSLA operating at 3.8 GHz. (c) Top view of the DBCCSLA. (d) Side view of the DBCCSLA. (e) Zoom view of capacitively coupled feeding section. (f) Fabricated prototype of the DBCCSLA.

IV. DUAL BAND CAPACITIVELY COUPLED SQUARE LOOP ANTENNA (DBCCSLA)

In Section III, the capacitive coupling and loading gaps are employed to develop thin square loop antenna with broad bandwidth. This concept is now further utilized for realizing a Dual Band CCSLA (DBCCSLA). For this, a design consisting

of two individual's co-centred CCSLA is pursued. One CCSLA is designed to resonate at 4.7 GHz and other with slightly bigger loop is designed for 3.8 GHz. The figure below shows how the two loops are integrated together on one antenna to form DBCCLA, whose lateral dimension is same as of previous designs at 80 mm × 80 mm.

Fig. 9 (a) and (b) shows the top views of the individual CCSLAs for the two centre frequencies. The loop with l_1=38.6 mm resonates at 4.7 GHz and the one with l_2=49.16 mm resonates at 3.8 GHz. The substrate dimensions of 80m × 80 mm and the antenna thickness of 3.04 mm are kept the same as in the previous designs. The values for other parameters obtained are w_1=1 mm, g_1 =2.3 mm, l_{p1} = 5.8mm, w_{p1}= 3.48 mm, g_{p1}=0.35 mm, d_1=0.9 mm, w_2=1 mm, g_2=2.3 mm, l_{p2} = 5.8 mm, w_{p2}= 2.68 mm, g_{p1}=0.6 mm and d_2=0.5 mm. For brevity the reflection coefficients and radiation patterns of these two individual antennas are not presented.

When the two square loops are co-centred and are fed using common patches, Fig 9 (c), the emerged antenna has dual band behaviour. However, the mutual coupling effect due to integration of the two loops causes a slight shift in the frequencies of the two operating bands. Thus, to bring the resonances back at 4.7 GHz and 3.8 GHz the dimensions of loops and feeding patches had to be re-optimized by using the Genetic Algorithm (GA) in the transient solver of CST Microwave Studio [16]. Fig. 9 (c), (d), (e) and (f) show the top, side, zoom and the experimental prototype views of the DBCCSLA with the optimized dimensions l_{in} =39.9 mm, l_{out} =49.36 mm, w =1 mm, g =2.7 mm. The two square loops are coupled with four rectangular common feeding patches (A_P, B_P, C_P and D_P) which are placed between the two loops. The centre of each patch is aligned with the centre of each adjacent loop arm. The inner and outer loops are separated from the patches by a distance of $g_{p,in}$=0.35 mm and of $g_{p,out}$=0.6 mm, respectively. Each of the patches has a length of l_p=5.5 mm and a width of w_p=2.78 mm. The patches are fed from the bottom via four vertical probes which are connected to the centre of the patch.
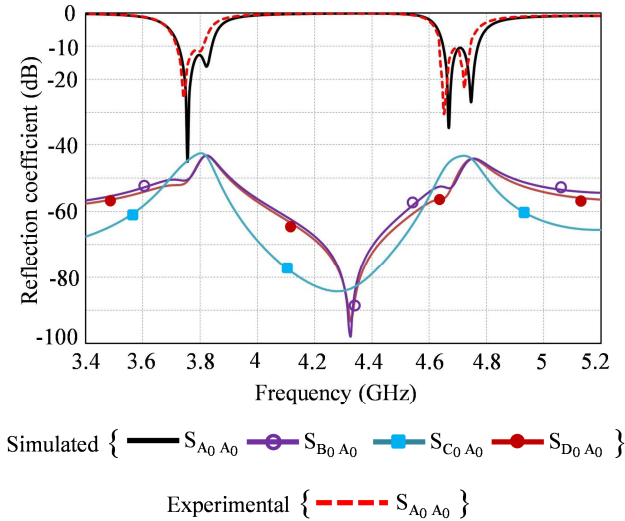
Fig. 10. Simulated and experimental reflection coefficient of the DBCCSLA.

Fig. 10 shows the simulated and experimental reflection coefficient of the DBCCSLA when port $A_{0,rf}$ is excited by an RF source and remaining ports (B_0, C_0 and D_0) are open circuited. The experimental results are in close agreement with the simulated results. Both the operating frequency bands of 4.7 GHz and 3.8 GHz have similar −10 dB impedance bandwidth of 120 MHz each. Note, this is half of 240 MHz that offered by CCSLA. Apparently, the introduction of the second loop in DBCCLA has increased the Q-factor of the antenna for each band by a factor of two, hence reducing the associated bandwidth by the same factor to 120 MHz. The isolations between the excited port A_0 and passive ports (B_0, C_0 and D_0) are well below -40 dB as shown in the Fig. 10. Due to the symmetry of the feeding ports with respect to the antenna structure the reflection coefficients and isolations of other ports are expected to be very close (or ideally identical) to that of port $A_{0,rf}$.

Fig. 11 shows the simulated three-dimensional radiation pattern along with the simulated and experimental two-dimensional cuts of the normalized radiation pattern at 4.7 GHz and 3.8 GHz. The measured results are in good agreement with the simulated results. In both bands, when port $A_{0,rf}$ is fed by an RF input and remaining ports are open circuited, the antenna generates a tilted beam pointing towards the opposite quadrant of excited port. As shown in the elevation cuts at 4.7 GHz the antenna generates a tilted beam of θ_{max} =31° towards the direction of ϕ_{max}=45°. The antenna has a maximum directivity of 9.3 dBi in the direction of maximum radiated field. Similarly, at 3.8 GHz the antenna radiates a tilted beam with the maximum radiated field located at θ_{max} =31°, ϕ_{max}=45° and has a slightly reduced directivity of 9.2 dBi. The radiation efficiency was found to be 81%. As expected, due to the flow of the current in a linear direction, the main lobes are linearly polarized in the E_θ direction and because of that the cross component has a very low magnitude ($E_\phi \leq -40$ dB), thus are not visible in the elevation cut. The azimuth cuts show cross polarized E_ϕ components but they are well under −9 dB from that of the co-polarized main beam. It is also noted that the cross polarized side-lobes have a null in the direction of the co-polarized main lobe. The main beams having a half power (3 dB) azimuth beam width of approximately 75°, which covers an almost entire space quadrant ($0 \leq \phi \leq 90°$) opposite of port $A_{0,rf}$. Since the dual square loop structure is symmetrical with the feeding ports, the radiation patterns of other ports (B_0, C_0 and D_0) are expected to be similar to that of port $A_{0,rf}$.

Therefore, in both bands, when each of the four ports is individually excited, keeping other ports open circuited, the antenna provides tilted beam of θ_{max} =31° in four different space quadrants of ϕ_{max}=45°, ϕ_{max}=135°, ϕ_{max}=225° and ϕ_{max}=315°. Thus, this beam can be steered over four quadrants to cover the entire space in front of the antenna by switching the RF input among the ports. This tilted beam in four quadrants of space is of special significance for indoor wireless communications where signals generally arrive from the sideways rather than the axial direction. The feed switching network for four beams can be implemented by PIN diode based RF switches as shown in [23].
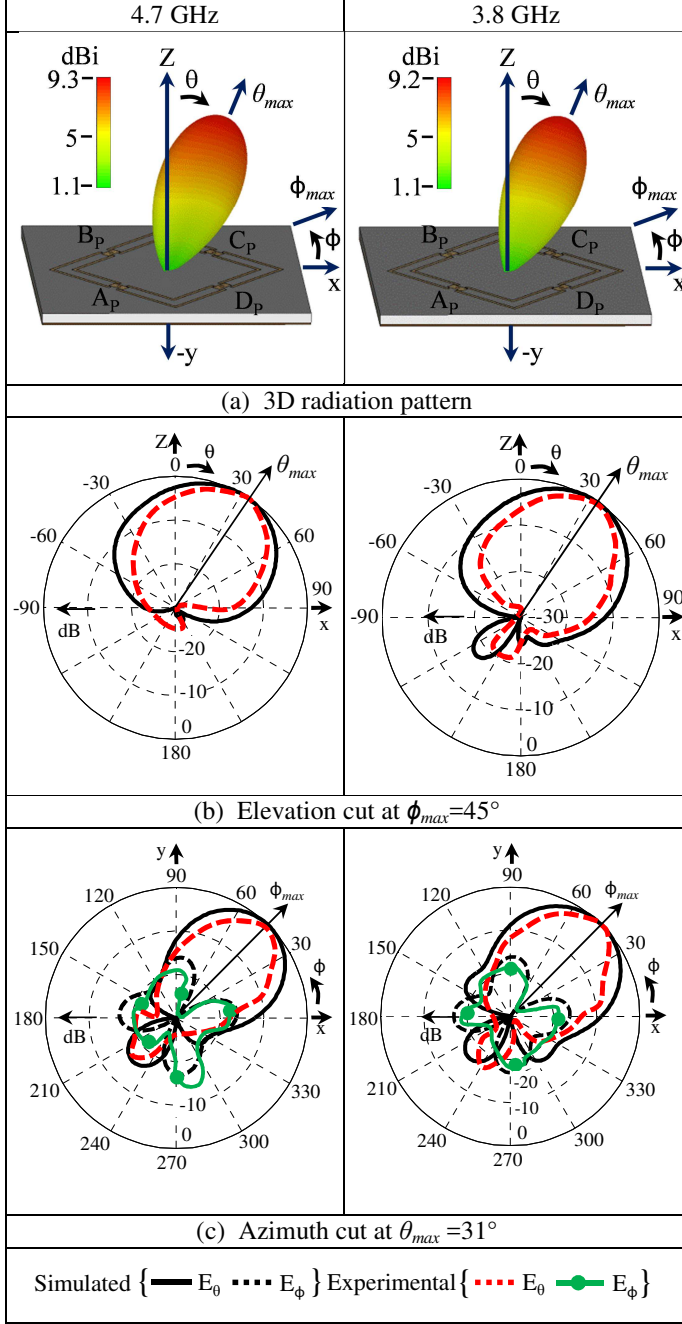
Fig. 11. Simulated and experimental radiation patterns of DBCCSLA at 4.7 GHz and 3.8GHz (a) three-dimensional, (b) elevation cut at ϕ_{max} = 45° and (c) azimuth cut at θ_{max} =31°.

It was found that the antenna provides tilted beam for both the operating frequency bands. Outside the frequency bands the patterns get distorted. Fig. 12 and Fig. 13 show the variation of the beam-tilt angle and directivity in the direction of maximum radiation over the operating frequency bands of 4.7 GHZ and 3.8 GHz, respectively. A variation of 0.8 dB (9.3-8.5 dBi) in maximum directivity and 25° (25°-50°) in beam-tilt angle is observed over the 4.7 GHz frequency band. On the other hand the maximum directivity varies from 7.3 dBi to 9.2 dBi (1.9 dB) over the 3.8 GHz frequency band and a variation of 22°

(23°-45°) in beam-tilt angle is notable. For both the bands, the beam tilt variation is consistent with our earlier findings on SLA [8]-[9] in where the beam tilt is smaller at the lower side of the resonance and is higher towards the upper end of the resonance. This is irrespective of the resonance bandwidth.
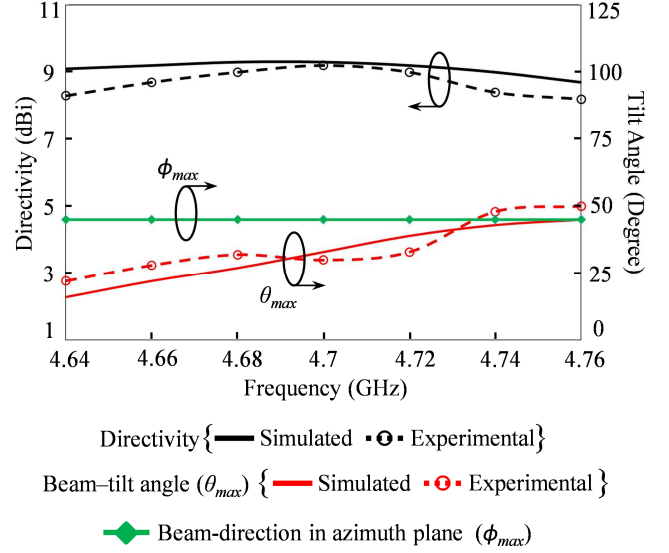
Fig. 12. Simulated and experimental beam-tilt angle and directivity of the antenna in the direction of the maximum radiation over the 4.7 GHz (4.64-4.76 GHz) frequency band.
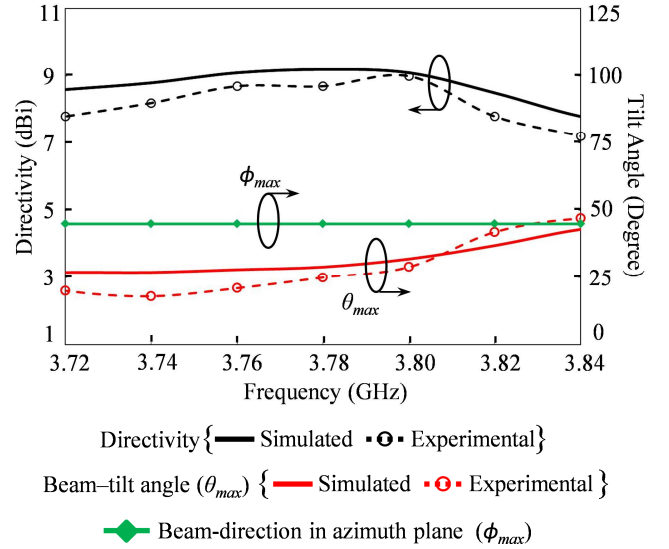
Fig. 13. Simulated and experimental beam-tilt angle and directivity of the antenna in the direction of the maximum radiation over the 3.8 GHz (3.72-3.84 GHz) frequency band.

V. CONCLUSION

Research and development towards achieving a low profile capacitively coupled square loop antenna for dual band beam steering applications was presented. The dual band antenna uses two co-centered square loops. It was demonstrated how a

capacitively coupled feeding arrangement can bring appropriate capacitance into the input impedance of the antenna to compensate for the high inductance generated due to close vicinity of the ground plane. This feeding mechanism allows the input impedance of the antenna to be matched easily to the 50Ω feed line and helps in the realization of the low profile SLA (3.04 mm at $\lambda_0/26$). Four narrow gaps were introduced in each square loop of the antenna to enhance the impedance bandwidth of the antenna by exploiting the loaded modes of the loop. The dual band antenna was designed and optimized for operating in the 4.7 GHz and 3.8 GHz bands. For both the bands the antenna has an impedance bandwidth of 120 MHz, and when one of its ports is excited and the remaining three ports are open circuited, the antenna generates a tilted beam (with 9.3 dBi_{max} directivity) pointing away from the excited port. Thus, the antenna can steer its tilted beam in four different quadrants by appropriately exciting one of the ports whilst keeping the remaining ports open circuited.

REFERENCES

[1] J. C. Liberti and T. S. Rappaport, Smart Antennas for Wireless Communications: IS-95 and Third-Generation CDMA Applications. Englewood Cliffs, NJ: Prentice Hall, 1999.

[2] D. Pozar, "Finite phased arrays of rectangular microstrip patches," *IEEE Trans.Propag.*, Vol 34, No. 5, pp. 658-665, May, 1986

[3] G. H. Huff , J. Feng , S. Zhang and J. T. Bernhard, "A novel radiation pattern and frequency reconfigurable single turn square spiral microstrip antenna," *IEEE Microw. Wireless Compon. Lett.*, vol. 13, pp. 57-59, Feb. 2003.

[4] A. Mehta and D. Mirshekar-Syahkal, "Spiral antenna with adaptive radiation pattern under electronic control," *IEEE AP-S Int. Symp.*, Monterey, CA, USA, pp. 843–846, Jun. 2004.

[5] A. Mehta, D. Mirshekar-Syahkal, and H. Nakano, "Beam adaptive single arm rectangular spiral antenna with switches," *IEE Proc.Microw., Antennas Propag.*, vol. 153, no. 1, pp. 13–18, Feb. 2006.

[6] C. W. Jung, M. Lee, G. P. Li, and F. De Flaviis, "Reconfigurable scanbeam single-arm spiral antenna integrated with RF-MEMS switches," *IEEE Trans. Antennas Propag.*, vol. 54, pp. 455–463, Feb. 2006.

[7] A.Pal, A.Mehta, D.Mirshekar and P.J.Messy, "Doughnut and Tilted beam generation using a single star patch antenna," *IEEE Trans. Antennas and Propagation*, vol. 57, no. 10, pp. 3413-34180, Oct. 2009.

[8] A. Mehta and D. Mirshekar-Syahkal, "Pattern steerable square loop antenna," *IEE Electronics Letter (IET),* vol. 43, no. 9, pp. 491-493, Apr. 2007.

[9] A. Pal, A. Mehta, D. Mirshekar-Syahkal and P.J.Messy, "Short-circuited feed terminations on beam steering square loop antennas," *IEE Electronics letter (IET),* vol. 44, no. 24, pp: 1389-1390, Nov. 2008.

[10] D. Sievenpiper, L. Zhang, R. F. J. Broas, N. G. Alexopolous, and E.Yablonovitch, "High-impedance electromagnetic surfaces with a forbidden frequency band," *IEEE Trans. MTT*, vol. 41, pp. 2059–2074, Nov. 1999.

[11] J. Yeo and R. Mittra, "Bandwidth enhancement of multiband antennas using frequency selective surfaces for ground plane," *in proc. IEEE AP-S Int. Symp.,* Boston, MA, 8-13, Jul. 2001.

[12] P.Deo, A.Mehta, D.Mirshekar-Syahkal, P.J.Messy and H.Nakano, "Thickness reduction and performance enhancement of steerable square loop antenna using hybrid high impedance surface," *IEEE Trans. Antennas Propag.*, vol 58, pp.1477-1485, May 2010.

[13] A. Pal, A. Mehta, D. Mirshekar-Syahkal, and H. Nakano, "Low profile steerable loop antenna with capacitively coupled feeds," *IEEE Antennas and Wireless Propag. Letter.*, vol.11, pp. 873-876, Jul. 2012.

[14] A. Pal, A. Mehta, D. Mirshekar-Syahkal, and H. Nakano, "Low profile capacitively fed steerable square loop antenna," *IEEE Antennas and Propag. Society Int. Symp. Digest,* Chicago, IL, USA, 8-14 Jul. 2012.

[15] S.I. Latif and L.Shafai, "polarization and resonant characteristics of gap-loaded microstrip square ring antennas," *IET Microwaves, Antennas & Propagation*, Vol. 4, no.6, pp. 733–742. Dec. 2008.

[16] CST *GmbH. Darmstadt,* version 2011, Germany, Available: http://www.cst.com

[17] StarLab, Satimo, Courtaboeuf, France.

[18] R. Garg, P. Bhatia, I.J.Bhal and A. Ittipiboon, *Microstrip antenna design handbook*, Artech House, Boston, 2001.

[19] F. Abboud, J. P. Damiano, and A. Papiernik, "Simple model for the input impedance of the coax-feed rectangular microstrip patch antenna for CAD," *Proc. Inst. Elect. Eng.*, vol. 135, no. 5, pp. 323–326, 1988.

[20] M. Kirschning, R. H. Jansen, Jansen, and N. H. L. Koster, "Measurement and computer aided modeling of microstrip discontinuities by an improved resonator method," *IEEE MTT-S Digest*, pp. 495–497, 1983.

[21] S. Hong and M. J. Lancaster, "Microstrip bandpass filter using degenerate modes of a novel meander loop resonator," *IEEE Microwave and Guided Wave Letters*, vol. 5, no. 11, pp.371-372, Nov. 1995.

[22] M.A.Sultan, "The mode features of an ideal-gap open-ring microstrip antenna," *IEEE Trans. Antennas Propag.*, vol 37,no. 2 pp.137-142, 1989.

[23] P.Deo, M.Pant, A.Mehta, D. Mirshekar-Syahkal and H. Nakano, "Implementation and simulations of commercial RF switch integration with steerable square loop antenna," *IEE Electronics Letter (IET)*, vol. 47, no. 12, pp: 686-687, Jun. 2011.